Mechanical and Acoustic Performance of Compression-Molded Open-Cell Polypropylene Foams

Joe D. McRae,[1] Hani E. Naguib,[1] Noureddine Atalla[2]

[1]*Department of Mechanical and Industrial Engineering, University of Toronto, Toronto, Canada*
[2]*Groupe d'Acoustique et de Vibrations de l'Université de Sherbrooke, Canada*

Received 17 March 2009; accepted 11 October 2009
DOI 10.1002/app.31581
Published online 17 December 2009 in Wiley InterScience (www.interscience.wiley.com).

ABSTRACT: Open-cell materials are lightweight and multifunctional capable of absorbing acoustic energy and supporting mechanical load. The acoustic and mechanical performance of open-cell materials can be optimized through processing. In this article, the relationships between processing parameters and acoustic and mechanical performance are shown for polypropylene (PP) foams. PP foam samples are fabricated using a combined compression molding and particulate leaching process. The results from a parametric study showed that both salt size and salt to polymer ratio affect the acoustic and mechanical performance of open-cell PP foams. As salt size increases, cell size increased and cell density decreased. The salt to polymer ratio had opposite affect on cell density, and increasing the salt to polymer mass ratio increased the open-cell content. The airflow resistivity decreased significantly by increasing the cell size, which means that foam samples with smaller cell size have better sound absorption. When foam samples were thin, smaller cell sizes produced better sound absorption; however, as thickness of the sample increases, medium cell size offered the best acoustic performance. The compressive strength of the foams was increased by increasing the relative density. Acoustic performance results from the parametric study were compared to the Johnson-Allard model with good agreement. Finally, optimal cellular morphologies for acoustic absorption and mechanical performance were identified. J Appl Polym Sci 116: 1106–1115, 2010

Key words: open-cell foam; polypropylene (PP); sound absorption; compression strength; computer modeling

INTRODUCTION

Compression molding has been widely used in the plastic industry to manufacture large parts such as automotive hoods, fenders, and spoilers.[1,2] The process is relatively inexpensive because of its simplicity and low waste.[3] The process is also capable of manufacturing large intricate parts with good surface finish.

Compression molding has been used to create open-cell polymer foams by many researchers. Fossey et al. combined solvent blending and particulate leaching with compression molding to create polyethylene foams.[4] Here, the solvent blending was critical to evenly disperse polyethylene throughout the salt particles. More recently, compression molding has been used to create open-cell bioscaffolds for tissue engineering.[5,6] Mooney and coworkers used a combined compression and gas foaming process to produce PLGA bioscaffolds.[5] In this process, samples are saturated with gas in a foaming chamber. When the pressure is released, a thermal instability is created in the polymer matrix and cells nucleate as gas escapes. Mooney and coworkers has shown that using carbon dioxide instead of nitrogen creates foams with greater porosity.[7]

In the noise control industry, three major methods are used to control unwanted noise: reducing sources of noise and vibration, using barriers to prevent sound and vibration from entering a controlled space, and applying sound absorbing materials to dissipate unwanted sound energy. The materials investigated in this article fit into the third method, dissipating unwanted sound energy. It is critical that these materials have open-cell networks that are interconnected with the ambient environment to absorb sound energy.

The acoustic performance of a material is measured by determining the fraction of energy absorbed by a sample when a plane wave is incident on its surface. This measurement, which can be conducted

Correspondence to: H. E. Naguib (naguib@mie.utoronto.ca).

Contract grant sponsor: Networks of Centers of Excellence of Canada; contract grant number: AUTO21.

Contract grant sponsors: Natural Science and Engineering Research Council of Canada (NSERC), Canada Research Chair (CRC), Canada Foundation of Innovation (CFI).

using an impedance tube, a plane wave is emitted from a loudspeaker and partially reflected by the sample to create a standing interference pattern in the tube. Two microphones are used to measure minimum and maximum sound pressure levels of the standing interference pattern. These pressures are used in

$$\alpha = 1 - \left(\frac{P_{max}/P_{min} - 1}{P_{max}/P_{min} + 1}\right)^2 \quad (1)$$

to calculate the sound absorption coefficient α, where P_{max} and P_{min} are the maximum and minimum sound pressures.[8] It is important to note that the sound absorption coefficient is not an intrinsic material property because it depends on the thickness and supporting method of the sample.

Modeling the sound absorption of porous materials with complex cell morphology is difficult. In the literature, three different approaches have been used: empirical models, analytical models, and finite element simulations. Delany and Bazley used empirical relationships between flow resistivity, wave number, and characteristic impedance to develop empirical model.[9] Two analytical models have been developed, the electro-acoustic analogy model and the Johnson Allard (JA) model. Lu et al. developed the electro-acoustic analogy model, where the acoustic system is modeled as an equivalent electric circuit of acoustic impedances.[10] Allard and Daigle developed an analytical model to describe the propagation and absorption of sound waves in porous media.[11] The JA model uses five macroscopic quantities: open porosity (ϕ), airflow resistivity (σ), tortuosity (α_∞), viscous and thermal characteristic lengths (Λ and Λ') to find the effective density (ρ), and effective bulk modulus (K) of the air fluid medium. In this model, the absorption coefficient (α) of the material is estimated as:

$$\alpha = 1 - |R|^2 \quad (2)$$

where, R is the reflection coefficient. Finally, finite element methods have also been used to model sound propagation in porous media. Recently, Atalla et al. have developed numerical models to represent poroelastic materials, composite acoustic materials, and multilayer porous materials.[12,13]

From the study using open-celled aluminum foam, it was investigated that the sound absorption capacity was improved by increasing the flow resistance and by using small pores and great foam thickness.[14] A comparative study of the acoustic impedance, absorption coefficient, and reflection coefficient of several thermoplastic porous compounds was presented by Soto et al.,[15] where it was shown that controlling the mean pore size and the type of cell would lead to an enhancement of the acoustic performance of thermoplastics materials. Imai and Asano[16] studied the effects of foam thickness, existence of air layer behind foam, and foam profiling on acoustic absorption of polyester-based and polyether-based flexible polyurethane foams. The objective of this article is to synthesize open-cell polypropylene (PP) foams using a compression molding and particulate leaching process and to characterize the foams. Through the use of particulate leaching techniques, the compression molding process is capable of fabricating open-cell foam materials. This method has not been used to create open-cell foams for acoustic applications. Hence, it is of great interest to investigate how processing affects open-cell foams made with this process. The relationships between processing parameters, cell morphology, acoustic performance, and mechanical properties will be examined.

DESIGN, FABRICATION, AND CHARACTERIZATION OF OPEN-CELL FOAM

Materials

The polymer selected to examine in this study is polypropylene (PP). PP was selected because of the weight saving, the low cost, and the environmental benefits it can provide to the automotive industry.[17,18] Specifically, the PP grade used in this study is Microthene FP 800-00 powder supplied by Equistar with density of 0.909 g/cm^3 and vicat softening and melting points of 150 and 163°C, respectively. The PP powder has a high melt flow index of 35 g/10 min measured in accordance with ASTM-D1238.[19] PP powder is spherical and supplied with 5 to 50 μm particles. Powder particles less than 106 μm in diameter were desired as they have better mechanical properties than foams made with larger particles.[20] Sodium chloride (NaCl) particles used in the salt leaching process were supplied by Fisher Scientific. The salt was sieved into 106–250, 250–500, and 500–850 μm particles.

Experimental setup

In this study, foam samples were produced using the process setup as shown in Figure 1. The batch setup consisted of two compression molds, one to produce acoustic samples and one to produce compression samples, a 24,000 lb Carver hydraulic press with 0–350°C heated temperature controlled platens, salt leaching containers, and 1125°C Fisher Scientific isotemp muffle furnace.

The compression molds were machined out of 6061 aluminum alloy. The acoustic sample mold produced a foam sheet of 147 mm long × 48 mm wide × 6.4 mm thick. The sheets produced were cut into

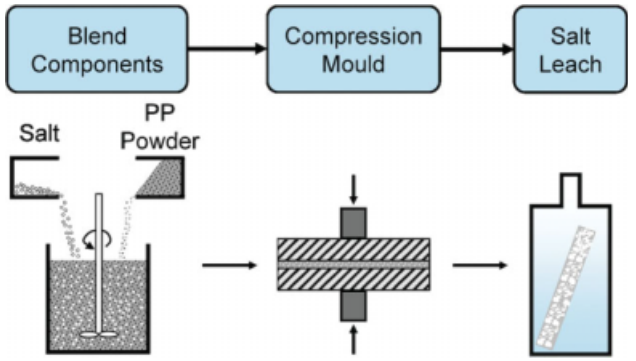

Figure 1 Batch foaming process. [Color figure can be viewed in the online issue, which is available at www.interscience.wiley.com].

four acoustic samples. The compression sample mold produced a 30 mm foam cube.

Fabrication procedure

The sample fabrication process can be divided into three main steps: dry-blending salt and polymer, compression molding the sample, and salt leaching to create an open-cell material. Unless otherwise stated the procedure was performed at room temperature and atmospheric conditions.

The mass of salt and polymer required to make each sample can be calculated using the following equations:

$$m_{\mathrm{PP}} = \frac{V_{\mathrm{geometric}} \times \rho_{\mathrm{NaCl}} \times \rho_{\mathrm{PP}}}{\rho_{\mathrm{NaCl}} + \rho_{\mathrm{PP}} \times r_{\mathrm{s/p}}} \tag{3}$$

$$m_{\mathrm{NaCl}} = \left(\frac{V_{\mathrm{geometric}} \times \rho_{\mathrm{NaCl}} \times \rho_{\mathrm{PP}}}{\rho_{\mathrm{NaCl}} + \rho_{\mathrm{PP}} \times r_{\mathrm{s/p}}}\right) \times r_{\mathrm{s/p}} \tag{4}$$

where $r_{\mathrm{s/p}}$ is the salt to polymer mass ratio and $V_{\mathrm{geometric}}$ is the geometric volume of the sample. In this study, the polymer was mixed with salt at different mass ratios and particle sizes by manually shaking a glass container of the mixture. Salt to polymer mass ratios of 4 : 1, 8 : 1, 12 : 1, and 16 : 1 and sieved salt particles of 106–250, 250–500, 500–850 μm were used. The PP and salt blend was transferred into a compression mold and heated at 180°C for 5 min on the compression press. The sample was then compressed at 7.5 MPa (1090 psi) for additional 5 min. The die was cooled to room temperature in a Fisher Scientific forma freezer at −35°C for 10 min. The molded samples were submerged in distilled water to leach for 96 h. The water was changed for every 24 h to avoid saturation. Finally, open-cell foam samples were created after the samples were dried for 24 h at 60°C. Finished open-cell foam samples fabricated with different salt sizes made for compression and acoustic testing are shown in Figure 2.

Characterization

Cross-section micrographs of the polymer foam were taken using a JOEL scanning electron microscope (JSM-6060). The cross-section images of foams were analyzed with ImageJ, image processing software developed by the National Institute of Health of USA, to determine average cell size and cell density. Cell density, N, is calculated using:

$$N = \left(\frac{n}{A}\right)^{3/2} \rho_r^{-1} \tag{5}$$

where n is the number of cells in the cross section image, A is the area of the image, and ρ_r, is the relative density.

Relative density is the ratio of the density of the foam, ρ^*, to the density of the bulk material, ρ, as defined below:

$$\rho_r = \frac{\rho^*}{\rho} \tag{6}$$

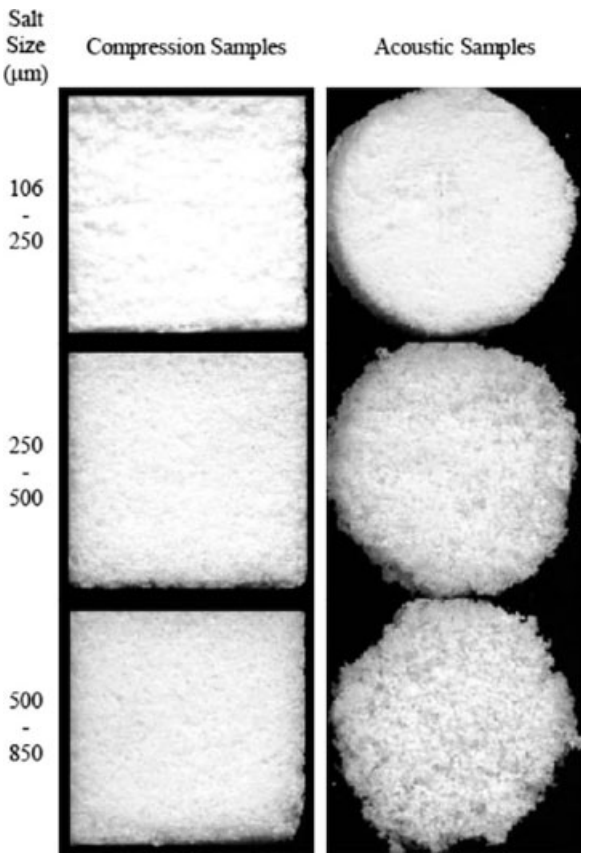

Figure 2 Polypropylene open-cell foam samples for compression and acoustic testing, processed with different salt sizes.

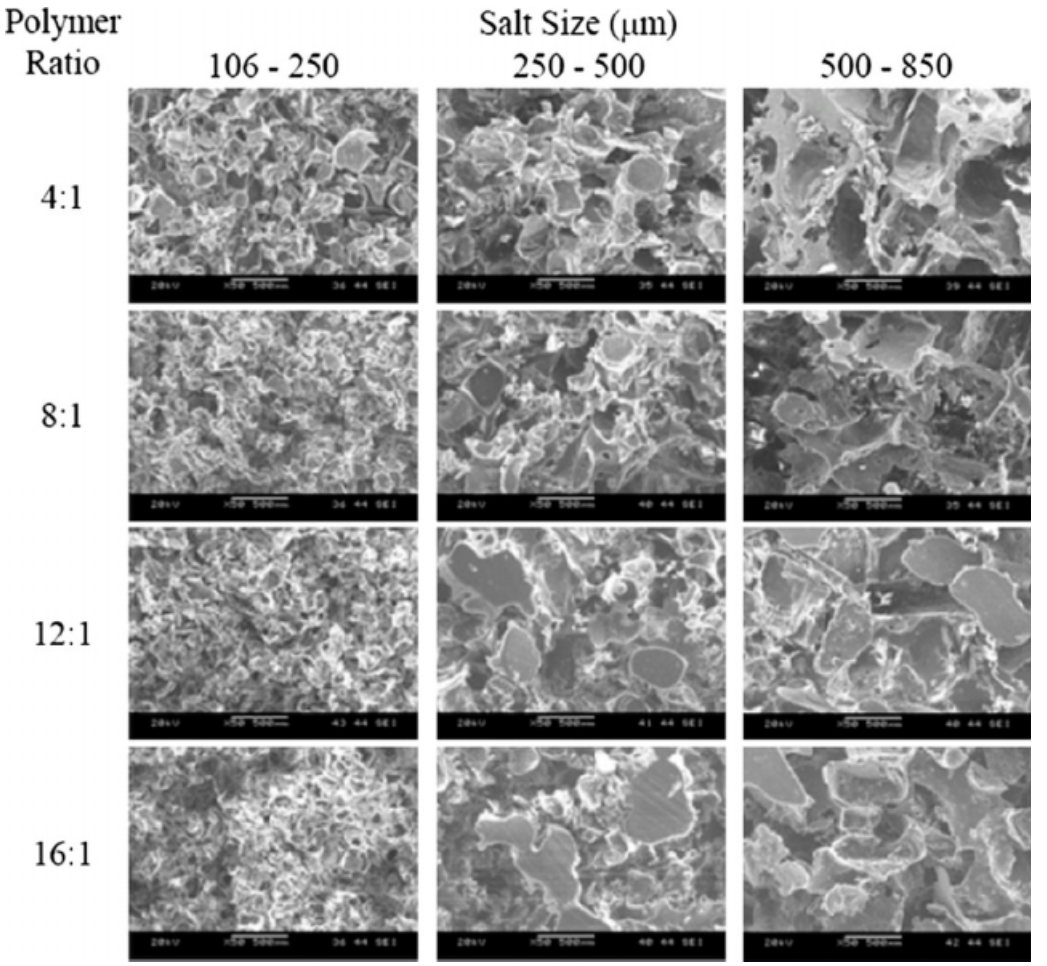

Figure 3 SEM images of cell morphology for different salt size and salt to polymer ratio.

The mass, the thickness, the width, and the length of foam samples were measured to calculate the foam density. Thickness, width, and length measurements were recorded as the average of three independent measurements. The mass of the samples was measured with a Denver instrument model P-214 electronic balance.

The open-cell content of a foam material is the percentage of the material that is interconnected with the ambient environment. The open-cell content was measured using UltraPync 1000 pycnometer by Quantachrome Instruments, which follows an American society for testing and materials (ASTM) standard, ASTM D6226.[21] The pycnometer pressurizes the foam sample with nitrogen at 6 psi and measures the closed-cell volume that cannot be penetrated by the pressurized nitrogen, V_{closed}. The open-cell content, O_V, is measured using:

$$O_V = \left(1 - \frac{V_{\text{closed}}}{V_{\text{geometric}}}\right) \times 100\% \quad (7)$$

The closed-cell volume percentage was also calculated using the pyncnometer measurements:

$$C_V = 100\% - O_V - \frac{m}{\rho_{\text{PP}} \times V_{\text{geometric}}} \times 100\% \quad (8)$$

The static airflow resistivity is measured with an airflow resistivity meter. The setup was built in accordance to the ASTM C522 standard.[22] Using the measured flow rate, U, and pressure difference, P, the airflow resistivity, σ, can be calculated as shown:

$$\sigma = \frac{P \times A}{U \times t} \quad (9)$$

The normal incident absorption coefficient, α, of the samples was measured at the University of Sherbrooke with a B&K Type 4206 impedance tube in accordance to ASTM 1050.[23] The impedance tube diameter was 29 mm, dictating an allowable frequency range of 50–6400 Hz. During testing, samples were wrapped with Teflon tape to seal gaps between the

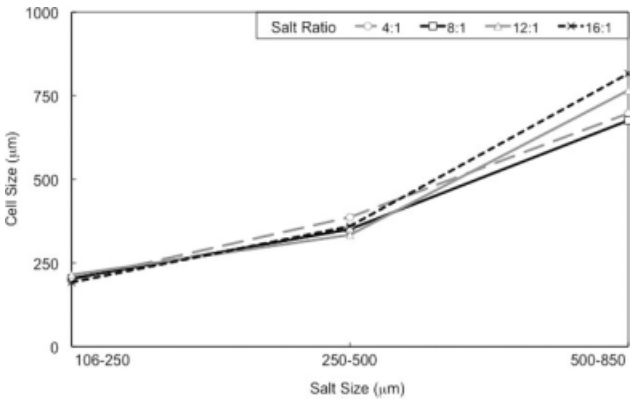

Figure 4 Effect of salt size on cell size.

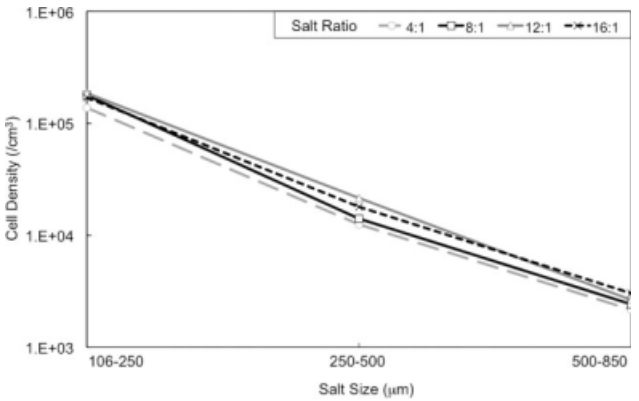

Figure 5 Effect of salt size on cell density.

sample holders and placed directly against a rigid impervious wall.

Mechanical properties of the foam samples were measured using a Shimadzu AG-I 50kN mechanical tester and an Instron 5548 500*N* micro tester. The polymer foam samples made with a 4 : 1 salt to polymer ratio were tested on the Shimadzu mechanical tester. The other polymer foam samples were tested on the Instron micro tester. Testing was done in accordance with ASTM D1621 with one deviation, and the values reported are for the average of three tests.[24] During testing, all samples were preloaded to 10N, and the tests were conducted at a strain rate of 2.5 mm/min. The stress–strain curves were analyzed to report Young's modulus and yield stress.

RESULTS AND DISCUSSION

Effect of salt characteristics on cell morphology

Salt parameters were varied during open-cell foam processing to determine the effect of processing parameters on cell morphology. Salt particle sizes of 106–250, 250–500, 500–850 μm and salt to polymer mass ratios of 4 : 1, 8 : 1, 12 : 1, and 16 : 1 were used. Cell morphology of the resulting samples was analyzed using scanning electron microscope images.

Cells are formed during the foaming process, when space is vacated by leached salt particles. Hence, the cell size and shape must be closely related to salt particles because both occupy the same space. Figure 3 shows SEM images of samples with varied salt to polymer mass ratio and salt size. The images clearly show that as salt size increases from 106–250 to 500–850 μm, the cell size increases. In Figure 4, the effect of increasing salt size is shown for each salt to polymer mass ratio.

Cell density, a measure of the number of cells in a given unit volume, was determined and is plotted against salt size in Figure 5. The cell density decreased with increasing salt size from 1.68×10^5 to 2.56×10^3 cells/cm^3. The salt to polymer ratio had a smaller and opposite affect on cell density; as the salt to polymer ratio increased from 4 : 1 to 16 : 1, the cell density increased 26% on average for each salt size. These results were expected because the cell density is closely related to the number of salt particle in a given sample. As salt size in a sample increases, the number of salt particles that can be packed into a given volume will decrease, thus decreasing the cell density. Increasing the salt to polymer mass ratio slightly increases the number of salt particles in a given sample, thus increasing the cell density.

In this study, the relative density of a sample will be proportional to bulk polymer mass because the volume is held constant. Salt particle size does not affect the relative density because it does not change the mass of polymer in each sample; however, the salt to polymer mass ratio, r_s, is expected to be inversely proportional to relative density:

$$\rho_r = \frac{1}{r_s} \tag{10}$$

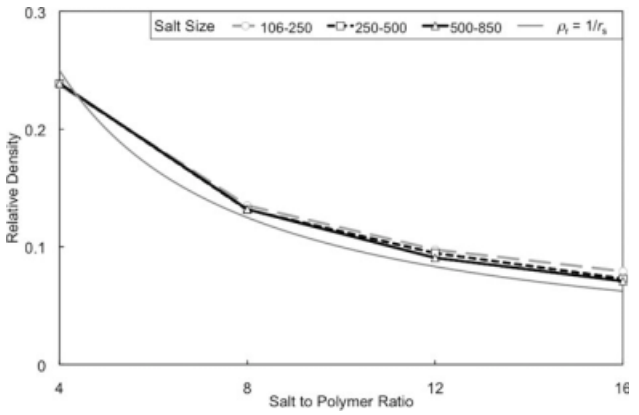

Figure 6 Effect of salt to polymer ratio on relative density.

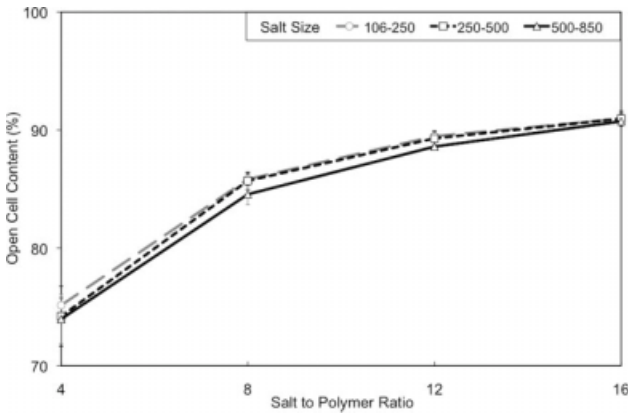

Figure 7 Effect of salt to polymer ratio on open-cell content.

As salt to polymer mass ratio increases from 4 : 1 to 16 : 1, the relative density decreases from 0.24 to 0.08. This relationship is shown in Figure 6.

Effect of salt characteristics on open- and closed-cell content

The open-cell content of foam is the percentage of the material that is interconnected with the ambient environment. Increasing the salt to polymer mass ratio from 4 : 1 to 16 : 1, increases the open-cell content to 17%, from 74 to 91%, as shown in Figure 7. Although the open-cell content measurement is useful in predicting acoustic performance, it does not succinctly describe the effectiveness of the open-cell foaming process. A better measurement to describe the performance of the foaming process is closed-cell content, which is the volume percentage of cells that are closed. Figure 8 shows the closed-cell content of foams produced with different salt to polymer ratios. The maximum closed-cell content for all samples was 2.2%, indicating the open-cell foaming process is effective.

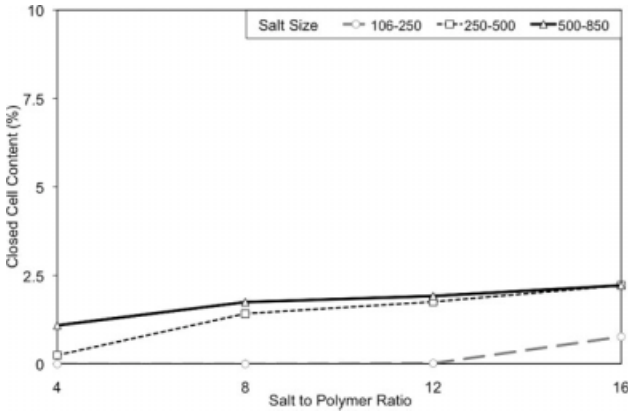

Figure 8 Effect of salt to polymer ratio on closed-cell content.

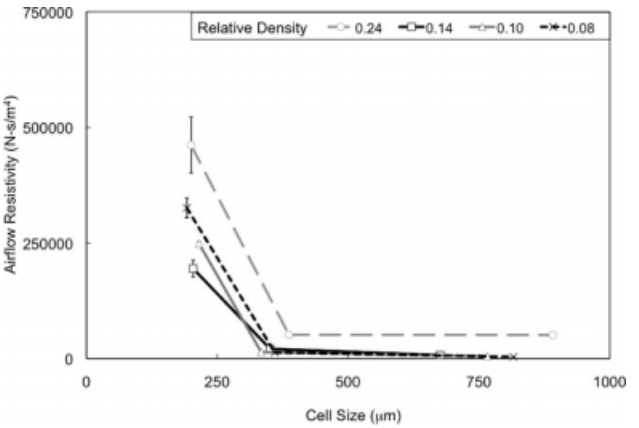

Figure 9 Effect of cell size on airflow resistivity.

Effect of cell morphology on static airflow resistivity

Static airflow resistivity was measured on each sample and effect of cell size is shown in Figure 9. The airflow resistivity decreases significantly from 3×10^5 to 2.5×10^4 N-s/m^4 by increasing the cell size from 106–250 to 250–500 μm. When increasing the cell size from 250–500 to 500–850 μm, the airflow resistivity decreased from 2.5×10^4 to 1.6×10^4 N-s/m^4. This trend can be explained by Allard, he estimated that the airflow resistivity is inversely proportional to the square of cell radius for foams with spherical cells[11]:

$$\sigma = \frac{8 \times \mu}{\phi \times r^2} \tag{11}$$

where μ is the dynamic viscosity of air.

Effect of cell morphology on sound absorption

In this study, 6.5 mm-disc samples were stacked together to investigate how cell morphology affects sound absorption of samples with different thickness. Samples with thicknesses of 6.5, 13, and 26 mm were examined in this study. Figure 10 shows sound absorption coefficient frequency spectra for 6.5, 13, and 26 mm samples produced with different cell size and 0.14 relative density. Results for other relative densities were similar.

The effect of thickness on sound absorption can be determined by comparing the graphs of 6.5, 13, and 26 mm sound absorption. As the thickness increases, the average sound absorption and the low frequency absorption of the sample both increase. This result is consistent with research conducted on polyurethane and aluminum open-cell foam.[25,26] The reason thicker foams have better sound absorption comes from the particle velocity theory described by Cox.[27] The theory states that significant sound absorption

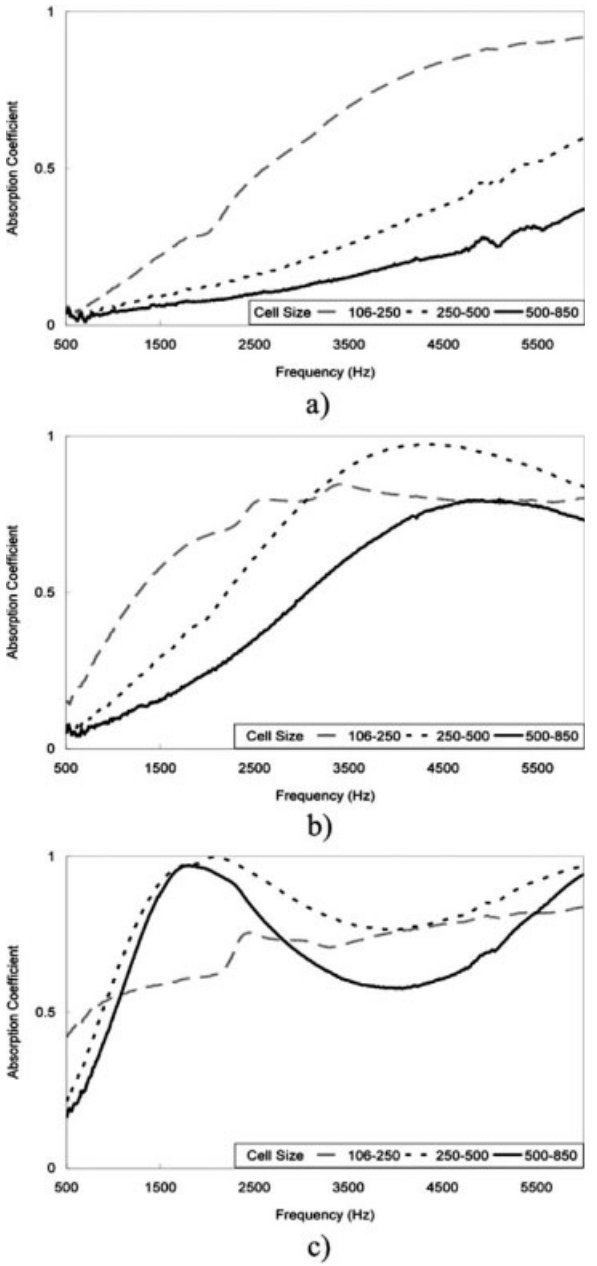

Figure 10 Effect of cell size on sound absorption frequency spectrums of (a) 6.5mm, (b) 13 mm, and (c) 26 mm samples.

only occurs where particle velocity is high. High particle velocity will occur in foam farthest away from the rigid wall boundary; hence, thicker samples should have better sound absorption.

The effect of cell size on sound absorption can be determined by comparing the curves on each individual graph in Figure 10. The 6 mm thick samples are better sound absorbers when the cell size of the foam is smaller. Samples produced with average cell sizes of 106–250, 250–500, and 500–850 μm had average sound absorption coefficients of 0.57, 0.26, and 0.18, respectively. Twelve millimetres thick samples demonstrated the same trend, average cell sizes of 106–250, 250–500, and 500–850 μm had average sound absorption coefficients of 0.70, 0.67, and 0.54, respectively. The 25 mm samples with average cell sizes of 106–250, 250–500, and 500–850 μm had average sound absorption coefficients of 0.71, 0.82, and 0.70, respectively. A medium cell size, 250–500 μm, offers the best acoustic performance in the 26 mm samples.

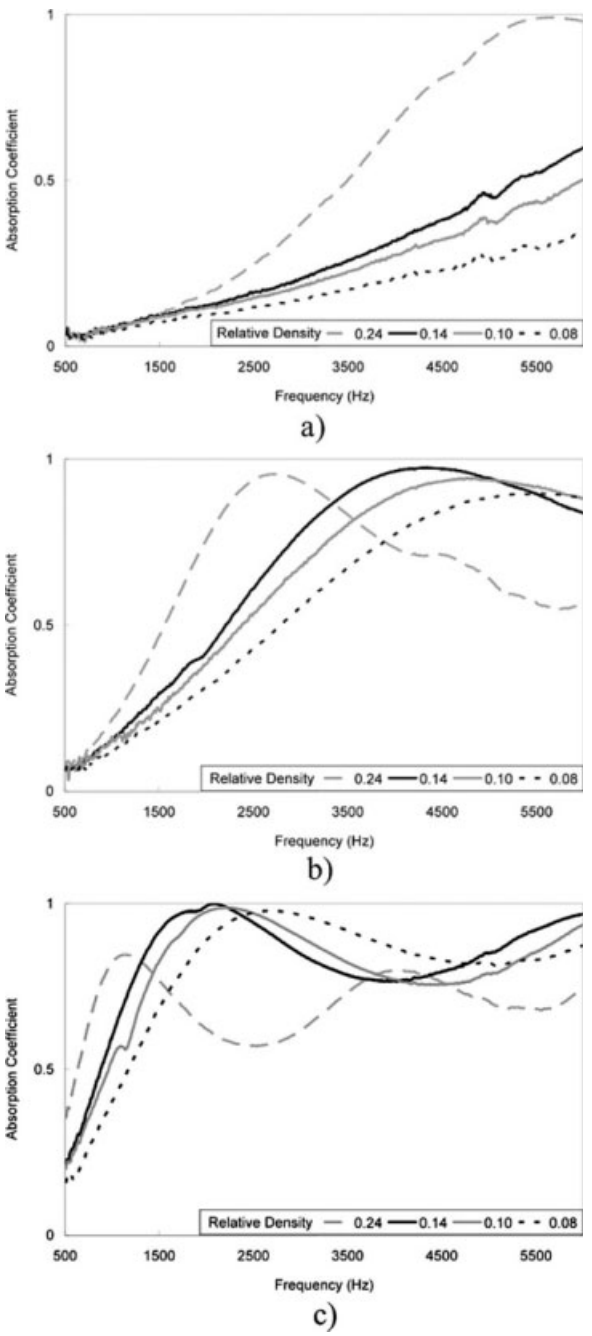

Figure 11 Effect of relative density on sound absorption frequency spectrums of (a) 6mm, (b) 13 mm, and (c) 25 mm samples.

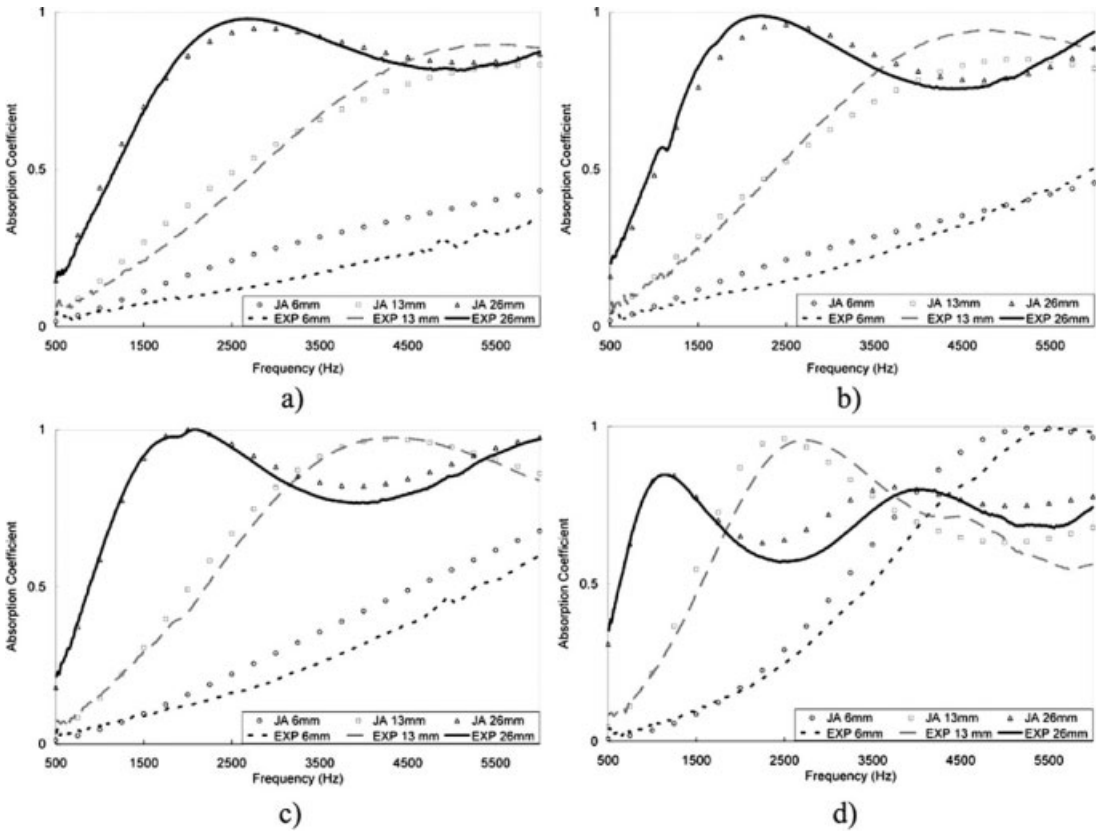

Figure 12 Johnson Allard modeling of sound absorption coefficient frequency spectrums of (a) 0.08, (b) 0.10, (c) 0.14, and (d) 0.24 relative density samples (JA, Johnson Allard; EXP, Experiment).

When foam samples were thin, less than 26 mm, small cell sizes produced the best sound absorption. However, as thickness of the sample increased to 26 mm, small cell sized samples had lower sound absorption than the medium and large cell sizes samples. This change in performance can be explained by the high airflow resistivity of the small samples. As the thickness of small cell sized samples increases, the difficulty for sound waves to travel in the cell structure also increases. This increase reduces the amount of sound energy that is dissipated in the cell structure.

Figure 11 shows sound absorption coefficient frequency spectrums for 6.5, 13, and 26 mm samples produced with different relative density and 250–500 μm cell size. Results for other cell sizes were similar.

The 6 mm thick samples are better sound absorbers when the relative density of the foam is higher. Samples produced with relative densities of 0.24, 0.14, 0.10, and 0.08 had average sound absorption coefficients of 0.48, 0.26, 0.23, and 0.17, respectively. Twelve millimetres thick samples demonstrated the same trend, samples with relative densities of 0.24, 0.14, 0.10, and 0.08 had average sound absorption coefficients of 0.65, 0.67, 0.63, and 0.56. The 25 mm samples with relative densities of 0.24, 0.14, 0.10, and 0.08 had average sound absorption coefficients of 0.70, 0.82, 0.80, and 0.79. The 0.14 relative density has the best performance in 26 mm samples. The relative density also affects the location of the maximum sound absorption peak. As the relative density decreases, the peak shifts to higher frequencies.

The effect of relative density can be explained by examining the surface layer of the open-cell foams. As the relative density decreases, the amount of cells per unit area on the surface increases. In thin samples, this change reduces the airflow resistivity and,

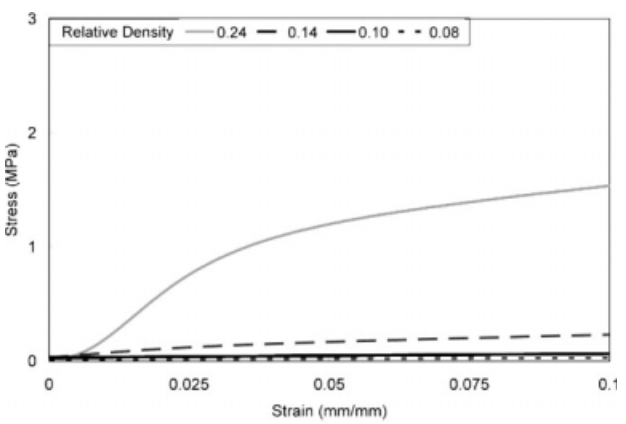

Figure 13 Compression stress strain plots for 106–250 μm cell size samples with different relative densities.

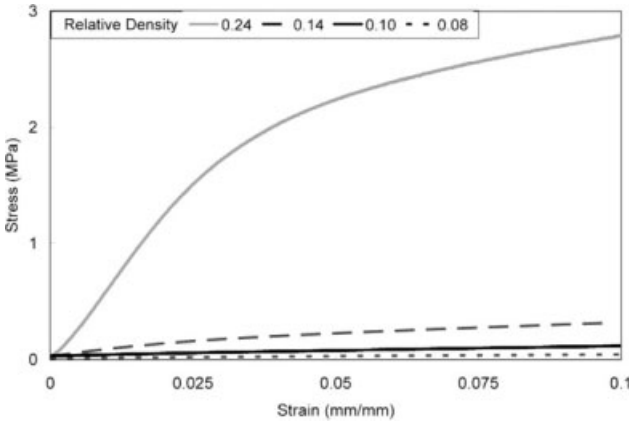

Figure 14 Compression stress strain plots for 250–500 μm cell size samples with different relative densities.

therefore, the absorption of sound energy in the sample. As the sample thickness increases, increasing the number of cell on the surface improves sound absorption, because less sound waves are being reflected back by solid material on the surface of the sample. This result is consistent with research conducted on porous magnesium.[28]

Modeling of sound absorption

In this section, the PP open-cell foam results shown in this article are compared with the JA model discussed earlier. The comparison will focus on the models ability to predict sound absorption of samples with different relative densities. Previous research conducted by Chu et al. shows the JA model accurately predicts sound absorption for open-cell PP foams with different cell sizes.[29]

Five inputs are needed for the JA model: porosity, airflow resistivity, tortuosity, and viscous and thermal characteristic length. For this comparison, the porosity and airflow resistivity were measured explicitly, and the remaining three parameters were

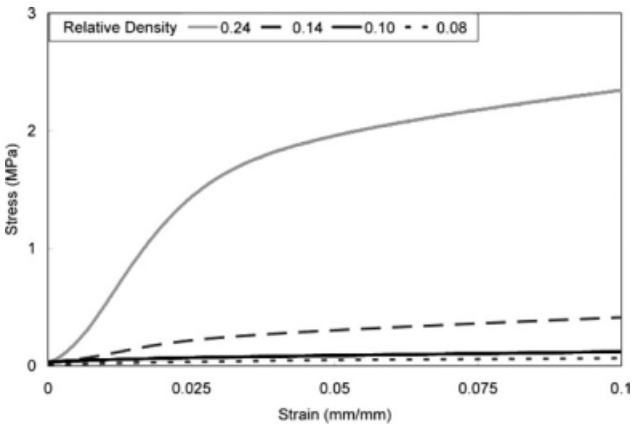

Figure 15 Compression stress strain plots for 500–850 μm cell size samples with different relative densities.

TABLE I
Mechanical Properties of Samples Produced with Different Cell Size and Relative Density

Relative density	Cell size (μm)	Young's Modulus (MPa)	Yield stress (MPa)
0.24	106–250	41.7	0.87
	250–500	72.9	2.20
	500–850	72.6	1.87
0.14	106–250	5.0	0.11
	250–500	7.4	0.14
	500–850	8.9	0.21
0.10	106–250	0.5	0.04
	250–500	1.3	0.07
	500–850	2.6	0.05
0.08	106–250	0.3	0.01
	250–500	0.7	0.03
	500–850	1.1	0.03

calculated using FoamX software. The software applies and inverse algorithm to sound absorption frequency spectrum data to calculate tortuosity and viscous, and thermal characteristic length.

The sound absorption behavior for samples with relative density from 0.08 to 0.24 was modeled and

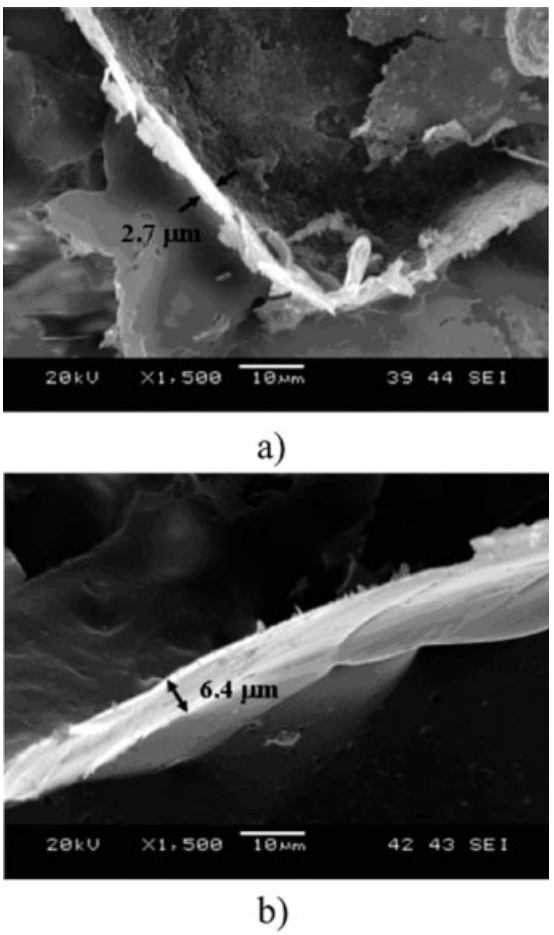

Figure 16 SEM images showing cell wall thickness of PP foam samples with relative densities of (a) 0.08 and (b) 0.24.

the results are shown in Figure 12. The experimental (EXP) and JA model sound absorption frequency curves shown in the figure have good agreement for all relative density and thicknesses. The average percent difference between experiment and the model was only 8% for average sound absorption. These results show that the JA model is capable of predicting sound absorption of open-cell PP foams.

Effect of cell morphology on mechanical properties

Compression stress–strain curves for different relative densities are shown below in Figures 13–15 for 106–250, 250–500, and 500–850 μm cell sizes. The values of Young's modulus and yield stress for these samples are given in Table I.

The figures show that increasing the relative density improve the compressive strength of the foams. Interpreting the results in Table I shows that increasing the relative density three times from 0.08 to 0.24 results in an average 100 times increase in Young's modulus and 75 times increase in yield stress. This exponential relationship is consistent with research conducted by Ashby on cellular materials.[30] Ashby applied elastic buckling theory to a 2D hexagonal unit cell and showed that relative density is the most important cellular parameter affecting mechanical properties. Relative density is the most important factor because it increases the mass of polymer, and therefore, the cell wall thickness increases, thus preventing buckling and improving mechanical properties.

SEM images of sample wall thickness from 0.08 to 0.24 relative density samples are shown in Figure 16. The SEM analysis clearly shows that the wall thickness of the 0.24 relative density sample is 3.7 μm (2.4 times) larger than the 0.08 relative density sample.

CONCLUSIONS

Open-cell PP foams with relative densities between 0.08 and 0.24 were produced using a compression molding/particulate leaching process. Good sound absorption with average absorption coefficients of 0.8 was achieved. Samples with relative densities of 0.24 combine an average absorption coefficient of 0.7 with great mechanical properties having a Young's modulus of 72.9 MPa and a yield stress of 2.2 MPa.

Results from the parametric study have shown foams made from small salt particles have smaller cells, larger cell densities, and higher airflow resistivity. These foams also make better sound absorbers where thin materials are required because as thickness increases they become too resistive and underperform samples with larger cell sizes. They will also have weaker mechanical properties because it is difficult for the polymer particles to flow and sinter in a matrix of small salt particles.

Foams made with lower salt to polymer ratio have higher relative density and lower open-cell content. These samples will make better thin sound absorbers because they are more resistive. They will also have the best mechanical properties because they have thicker cell walls.

Good agreement was shown between EXP results and the JA model for PP open-cell foams with relative densities between 0.08 and 0.24.

References

1. Isayev, A. I. Injection and Compression Molding Fundamentals; Marcel Dekker Inc.: New York, 1987.
2. Vlachopoulos, J.; Strutt, D. Mater Sci Technol 2003, 19, 1161.
3. Ebewele R. O. Polymer Science Technology; CRC Pr I Llc: Boca Raton, Florida, 2000.
4. Fossey, D. J.; Smith, C. H. J Cell Plast 1973, 9, 268.
5. Harris, L. D.; Kim, D. S.; Mooney, D. J. J Biomed Mater Res 1998, 42, 396.
6. Leung, L.; Chan, C.; Song, J.; Tam, B.; Naguib, H. E. J Cell Plast 2008, 44, 189.
7. Sheridan, M. H.; Shea, L. D.; Peters, M. C.; Mooney, D. J. J Control Release 2000, 64, 91.
8. Zwikker, C.; Kosten, C. W. Sound Absorbing Mater; Elsevier: New York, 1949.
9. Delany, M. E.; Bazley, E. N. App Acoust 1969, 13, 105.
10. Lu, T. J.; Hess, A.; Ashby, M. F. J App Phys 1999, 85, 7528.
11. Allard, J. F.; Daigle, G. J Acoust Soc Am 1994, 95, 2785.
12. Atalla, N.; Sgard, F. J Sound Vib 2007, 303, 195.
13. Atalla, N. Symposium on the Acoustics of Poro-Elastic Materials (SAPEM, 2005), Lyon, France, December 7–9, 2005.
14. Han, F.; Seiffert, G.; Zhao, Y.; Gibbs, B. J Phys D Appl Phys 2003, 36, 294
15. Soto, P. F.; Herrfiez, M.; Gonzfilez, A.; de Saja, J. A. Polym Test 1994, 13, 77.
16. Imai, Y.; Asano, T. J Appl Polym Sci 1982, 27, 183.
17. Liu, X.; Sun, Y. Hecheng Shuzhi Ji Suliao/China Syn Resin Plast 2005, 22, 75.
18. Kanari, N.; Pineau, J. L.; Shallari S. JOM 2003, 55, 15.
19. ASTM D 1238, American Society for Testing and Materials: Philadelphia, Pennsylvania, 2004.
20. Riddle, K. W.; Mooney, D. J. J Biomater Sci Poly Ed, 2004, 15, 1561.
21. ASTM D 6226, American Society for Testing and Materials: Philadelphia, Pennsylvania, 1998.
22. ASTM C 522, American Society for Testing and Materials: Philadelphia, Pennsylvania, 1997.
23. ASTM E 1050, American Society for Testing and Materials: Philadelphia, Pennsylvania, 2007.
24. ASTM D 1621, American Society for Testing and Materials: Philadelphia, Pennsylvania, 2000.
25. Tsay, H. S.; Yeh, F. H. J Cell Plast 2005, 41, 101.
26. Hakamada, M.; Kuromura, T.; Chen, Y.; Kusuda, H.; Mabuchi, M. Appl Phys Lett 2006, 88, 254106.
27. Cox, T. J.; D'Antonio, P. Acous Absorbers and Diffusers: Theory, Design, and Application; Spon Press: London, New York, 2004.
28. Xie, Z. K.; Ikeda, T.; Okuda, Y.; Nakajima, H. Mater Sci Forum 2004, 449, 661.
29. Chu, R. K. M.; Naguib, H. E.; Atalla, N. SPE ANTEC Technical Papers, Society of Plastics Engineers, Milwaukee, Wisconsin 2008.
30. Ashby, M. F.; Medalist, R. F. M. Metall Mater Trans A, 1983, 14, 1755.